CHAPTER 8

Filters

For our purposes, a filter is any electrical network through which passes a complex time-varying signal $F(t)$ and acts on this signal to selectively alter its harmonic makeup.

Fourier's theorem was briefly mentioned at the beginning of Chapter 3. The theorem shows how any periodic waveform $[F(t+T) = F(t)]$ can be synthesized from a sum of appropriately chosen harmonics of the fundamental periodicity $[\omega_n = n\omega_0 = n\frac{2\pi}{T}]$. Because of this, any signal may be thought of in terms of its equivalent Fourier spectrum—the frequency distribution of amplitudes C_n and phase shifts θ_n as implied by Eq. (3.4).

A filter, then, effectively modifies the C's and θ's in some prescribed manner. The standard filter categories are: low-pass, high-pass, band-pass, and band-stop.

As the names suggest (see Fig. 8.1), certain frequencies are either blocked or passed through.

From an instrumentation point of view, there are many reasons for filtering a raw signal. A common motivation is the need to remove noise. Because noise is typically broadband and particularly noticeable at high frequencies, carefully chosen low-pass filtering can clean up the signal in situations where the information content is primarily at the low end of the spectrum. Low-pass filtering can also reveal slow trends that may be masked by clutter at higher frequencies. Band-pass filters can be useful in isolating a specific frequency interval within which some phenomenon is expected to occur, such as mechanical resonances in a vibrating structure monitored by strain gages.

Ideal filters usually have abrupt transitions ("brick walls") at the edges of pass and stop bands. That is, frequencies are either completely passed through or totally blocked. Such perfection can never be achieved in practice. Designs that manage to produce relatively sharp transitions in the frequency domain are accompanied by ripple just below and just above the edge. The sharper the

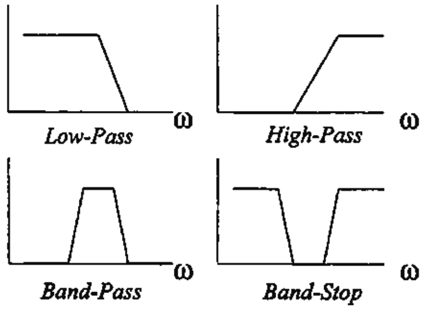

FIGURE 8.1. Four filter types: low-pass, high-pass, band-pass, and band-stop.

transition, the more the ripple. Improved sharpness without increased ripple can only be achieved with increased complexity in the filter design and with the addition of more reactive components to the filter (higher "order"). The essence of filter design is in balancing the tradeoffs between these competing factors and in assessing which attributes are most important for a given instrumentation application.

Electrical filters constructed entirely from resistors, capacitors, and inductors are termed *passive*, in contrast to filters employing transistors or op-amps, which are *active*.

8.1 PASSIVE FILTERS

Passive filters can be assembled from as few as two components, although increasingly complex designs permit more precise control of the frequency response.

First-Order Filters

Low-pass RC filter

Consider a series RC circuit as shown in Fig. 8.2. The voltage across the capacitor is given by the complex expression

$$\frac{V_{\text{cap}}}{V_{\text{in}}} = \frac{I\left(\frac{-j}{\omega C}\right)}{I\left(R + \frac{-j}{\omega C}\right)}, \tag{8.1}$$

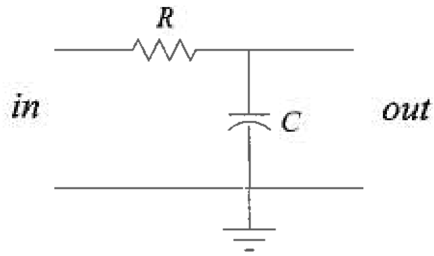

FIGURE 8.2. First-order low-pass RC filter.

where I is the ac current flowing around the loop and V_{in} represents the input source voltage. This equation may be arranged to

$$\frac{V_{\text{cap}}}{V_{\text{in}}} = \frac{1}{1 + j\omega CR} \tag{8.2}$$

or, in complex form with amplitude and phase,

$$\frac{V_{\text{cap}}}{V_{\text{in}}} = A\, e^{j\phi}. \tag{8.3}$$

In this equation,

$$\boxed{A = \frac{1}{\sqrt{1 + \omega^2 C^2 R^2}}} \tag{8.4}$$

and

$$\boxed{\phi = -\tan^{-1}(\omega CR)}. \tag{8.5}$$

Two limits are of interest. At low frequency, $A \simeq 1$, whereas at high frequencies $A \to (\omega CR)^{-1}$.

In the section on frequency response in Chapter 5, the concept of decibels was introduced. In these units, the limits are $A \simeq 0$ dB, and $A \to -20\ \log(\frac{\omega}{\omega_c})$ dB. The corner frequency is defined as

$$\boxed{\omega_c = \frac{1}{RC}}. \tag{8.6}$$

As an example, let $R = 1$ kΩ and $C = 0.1\ \mu$F. Then, $\omega_c = 10^4$ radians/sec, which corresponds to a corner frequency of $f_c = 1592$ Hz. PSpice results are plotted in Fig. 8.3, where this corner point is marked with a solid square. Note

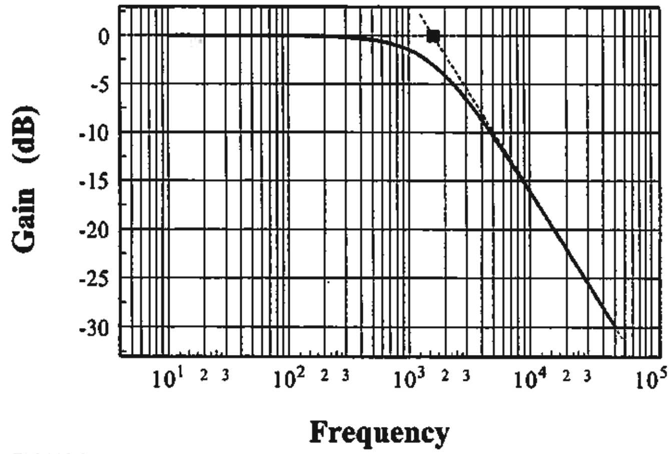

FIGURE 8.3. Frequency response for the RC low-pass filter. The vertical scale is logarithmic (decibels).

that at f_c the first-order response (gain) has dropped by 3 dB. The nearly linear rolloff well above f_c is quite apparent.

Clearly, this simple RC network functions as a low-pass filter. Well below the corner frequency, there is almost no attenuation of the input. Note, however, that there is no abrupt cutoff, but rather high frequencies are increasingly attenuated at the rate of 20 dB per decade. This means that any jump in frequency by a factor of 10 is accompanied by a matching drop of amplitude also by a factor of 10. This rate of 20 dB per decade can also be stated in equivalent terms as a rolloff of 6 dB per octave, an octave being any frequency jump by a factor of 2. These attenuation features are characteristic of a so-called *first-order* response.

Equation (8.5) describes the frequency-dependent phase shift that accompanies the filter attenuation. This behavior for the same PSpice simulation is illustrated in Fig. 8.4. In the limit $\omega \to 0$, the phase shift approaches zero. At high frequencies, this equation yields $\phi \to -90$ degrees. The negative sign in the phase angle indicates that the output from the low-pass filter lags the input. At the corner frequency of 1592 Hz, the phase shift is -45 degrees.

Low-pass RL filter

A simple two-component first-order low-pass filter can also be constructed from a resistor and an inductor. In this case, the positions of resistor and inductor are as illustrated in Fig. 8.5.

An analysis similar to that of the preceding section leads to the expression

$$\frac{V_R}{V_{\text{in}}} = \frac{1}{1 + j\,\frac{\omega L}{R}} \tag{8.7}$$

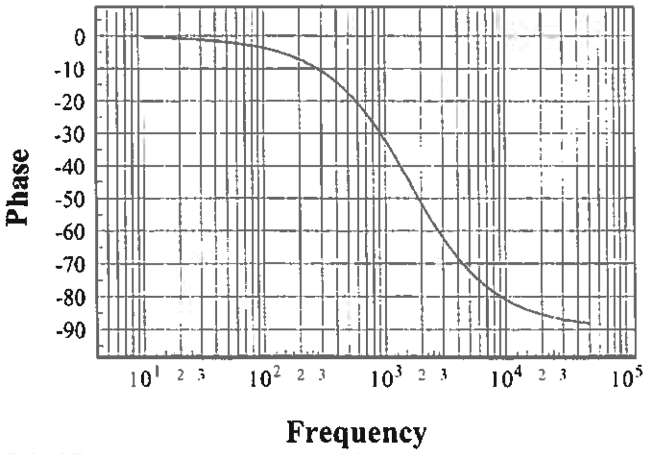

FIGURE 8.4. Phase response of first-order low-pass RC filter.

and thus

$$\frac{V_R}{V_{\text{in}}} = A\, e^{j\phi}, \tag{8.8}$$

with

$$\boxed{A = \frac{1}{\sqrt{1 + \frac{\omega^2 L^2}{R^2}}}} \tag{8.9}$$

and

$$\boxed{\phi = -\tan^{-1}\left(\frac{\omega L}{R}\right)}. \tag{8.10}$$

The corner frequency will be

$$\boxed{\omega_c = \frac{R}{L}}. \tag{8.11}$$

As an example, let $R = 1\ \text{k}\Omega$ and $L = 0.1$ H. This choice will set the corner frequency at the same value, $f_c = 1592$ Hz, as for the previous RC filter. It is

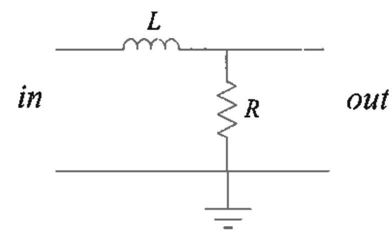

FIGURE 8.5. First-order low-pass LR filter.

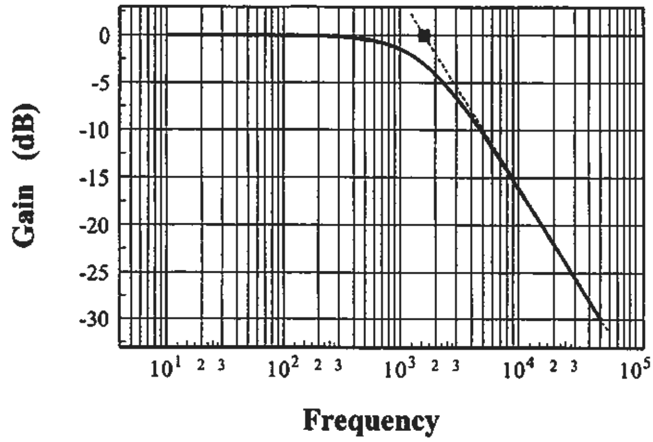

FIGURE 8.6. Frequency response of the RL filter.

immediately evident in the PSpice simulation results of Fig. 8.6 that the response characteristics of a low-pass *RL* filter are identical to those of a low-pass *RC* circuit (Fig. 8.3).

High-pass RC filter

Suppose the two components in the circuit of Fig. 8.2 are interchanged as in Fig. 8.7. The output voltage taken across the resistor is

$$\frac{V_R}{V_{\text{in}}} = \frac{1}{1 - \frac{j}{\omega CR}}. \tag{8.12}$$

As in the previous cases, let

$$\frac{V_R}{V_{\text{in}}} = A\, e^{j\phi}. \tag{8.13}$$

Then,

$$\boxed{A = \frac{1}{\sqrt{1 + \frac{1}{\omega^2 C^2 R^2}}}} \tag{8.14}$$

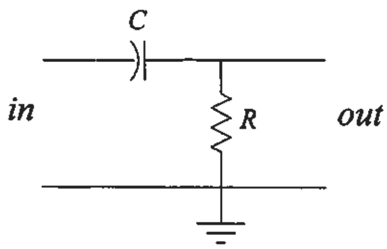

FIGURE 8.7. First-order high-pass RC filter.

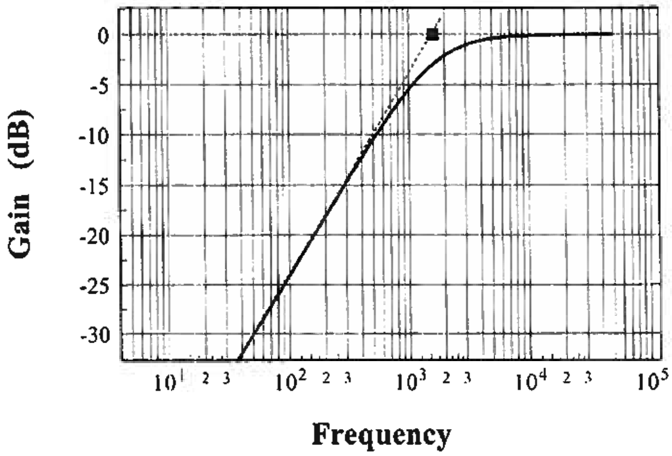

FIGURE 8.8. Frequency response of the first-order high-pass filter. As with the low-pass characteristic, the response is down 3 dB at the corner frequency.

and

$$\boxed{\phi = \tan^{-1}\left(\frac{1}{\omega CR}\right)}. \tag{8.15}$$

These two expressions can be compared to Eqs. (8.4) and (8.5), which applied to the low-pass filter. Note that in the present situation, the limits are the reverse of those previously found—that is, now at high frequencies $A \simeq 1$, whereas in the limit of low frequencies $A \to \omega CR$, which drops towards zero. Data from a PSpice simulation with $R = 1\ \mathrm{k}\Omega$ and $C = 0.1\ \mu\mathrm{F}$ are plotted in Fig. 8.8, where it is clear that this is a high-pass filter with the same corner frequency $\omega_c = \frac{1}{RC}$ as for the earlier low-pass circuit (see Fig. 8.3).

The phase shift as expressed by Eq. (8.15) approaches 90 degrees as $\omega \to 0$ and drops towards zero at very high frequencies, as if the curve in Fig. 8.4 were displaced vertically by 90 degrees. Because the phase factor ϕ is positive, the output from the high-pass filter leads the input.

Band-pass filter

It is readily apparent that a bandpass filter can be simply constructed from the product of suitable low-pass and high-pass filters, as indicated in Fig. 8.9. To illustrate this procedure, consider the circuit shown in Fig. 8.10.

Here, a high-pass filter made up of R_1 and C_1 is followed by a low-pass filter made up of R_2 and C_2. The order of the two does not matter. To choose a specific example, let $R_1 = 1$ K, $C_1 = 1.0\ \mu$F, $R_2 = 1$ K, and $C_2 = 0.1\ \mu$F. In this case,

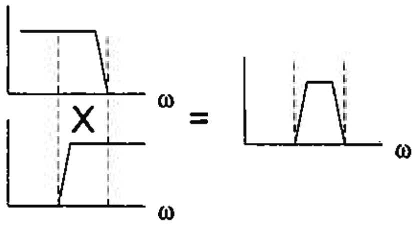

FIGURE 8.9. Synthesis of a band-pass filter from the product of a low-pass filter and a high-pass filter.

the lower corner frequency is set by the high-pass relationship

$$f_{cL} = \frac{1}{2\pi R_1 C_1} = 159.2\ \text{Hz},$$

and the upper corner point determined from the low-pass components is at

$$f_{cU} = \frac{1}{2\pi R_2 C_2} = 1592\ \text{Hz}.$$

A PSpice simulation produced the data plotted in Fig. 8.11. The expected band-pass behavior is clearly evident with dropoffs of 20 dB per decade at low and high frequencies.

The resulting phase shift from this composite filter is seen in Fig. 8.12. Because of the series connection, the phase shifts from each of the two filter blocks will simply add. Thus, it is expected that the overall phase shift of the band-pass design will be the sum of the phases expressed by Eqs. (8.5) and (8.15). At low frequencies, the phase-shifting properties of the high-pass filter dominate, while at high frequencies the phase shift is controlled by the low-pass section. As the figure demonstrates, below the passband midpoint the filter output signal leads the input signal; above the passband midpoint, the opposite is true. The

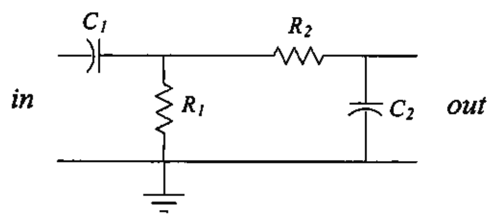

FIGURE 8.10. First-order band-pass filter using a combination of low-pass and high-pass sections.

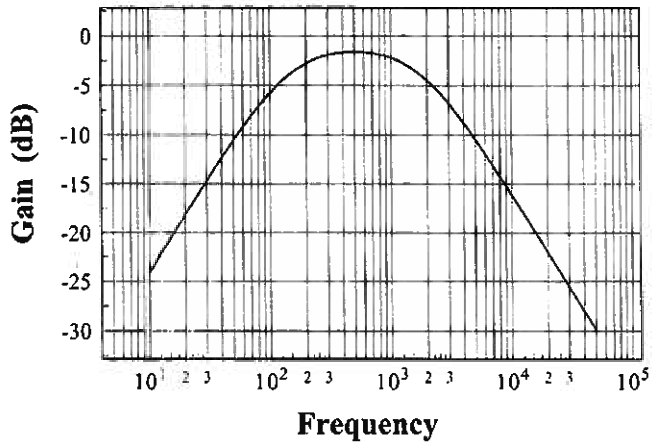

FIGURE 8.11. Frequency response of the band-pass filter.

neighborhood near the center of the passband is characterized by small phase shifts—clearly a desirable attribute.

Band-stop filter

The idea underlying the band-pass design was illustrated in Fig. 8.9. The product (series connection) of a low-pass and a high-pass filter generates an overall band-pass characteristic. A similar argument shows that a sum (parallel connection) of a low-pass module and a high-pass module can create a band-stop design, as suggested in Fig. 8.13.

In principle, this is straightforward, but in practice there is a complication. This arises from the need for an electronic summing operation to link the two filters.

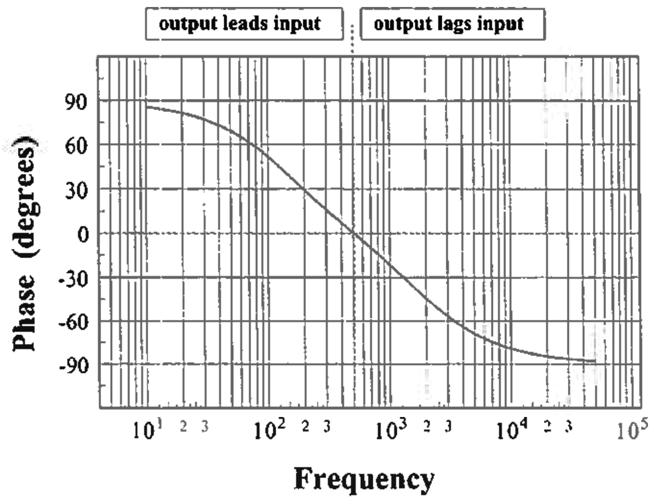

FIGURE 8.12. Phase response of the band-pass filter.

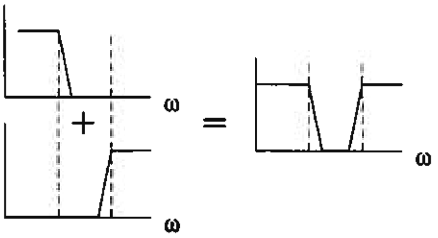

FIGURE 8.13. Synthesis of a band-stop filter from the sum of a low-pass filter and a high-pass filter.

But recall the summing amplifier (see Fig. 5.10) that was discussed in Chapter 5. As illustrated by the example in Fig. 8.14, this circuit allows the realization of the band-stop function. The combination R_1, C_1 is a low-pass first-order filter, whereas R_2 and C_2 comprise a high-pass first-order filter. The filter outputs are buffered by $U1A$ and $U2A$ and then summed by $U3A$. The corner points $f_c = (2\pi RC)^{-1}$ for these two filters are, for this example, 15.92 Hz and 3183 Hz, respectively. PSpice simulation results are shown in Fig. 8.15.

Note that for this plot a linear rather than logarithmic (decibel) amplitude scale has been chosen. This more clearly indicates the connection between the low-pass, high-pass, and band-stop (sum) characteristics. The center frequency of this filter is 226 Hz.

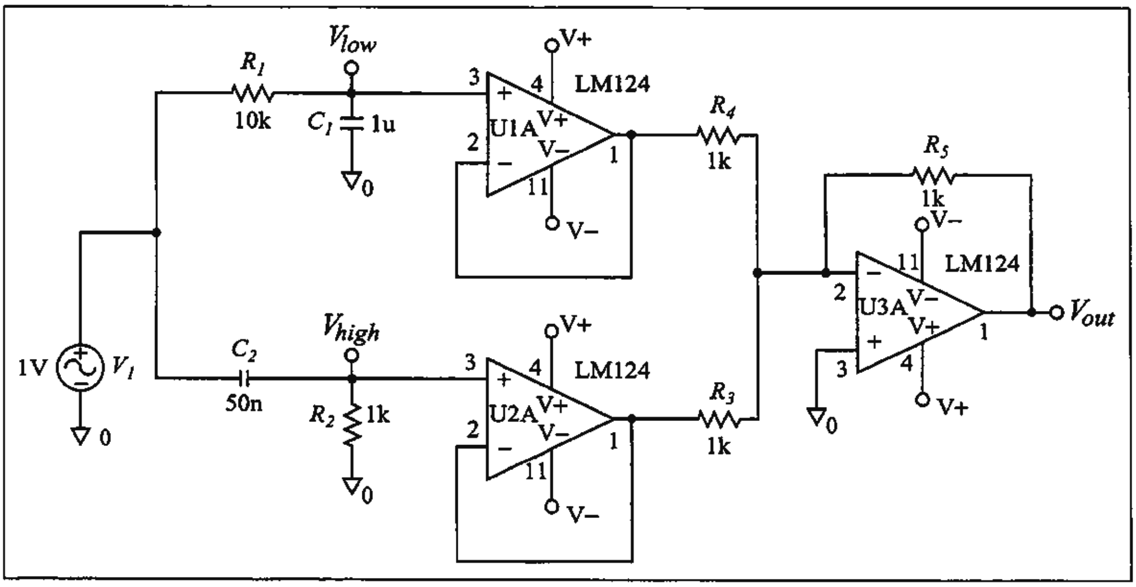

FIGURE 8.14. PSpice schematic showing a low-pass filter and a high-pass filter being combined in a summing amplifier to form a band-stop filter.

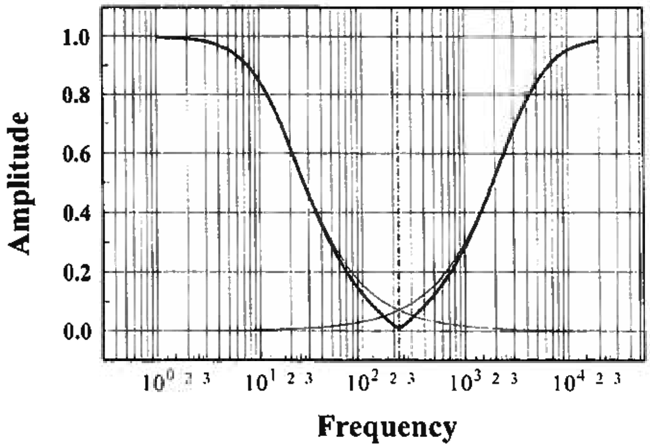

FIGURE 8.15. PSpice results for the band-stop filter.

Second-Order Filters

Cascaded filters

The band-pass filter discussed earlier was composed of a pair of *RC* units connected in series to form a composite network. It is, of course, possible to chain together any number of filter modules, just as one may chain together amplifier modules to increase gain. Suppose we have a series array of elements as depicted in Fig. 8.16.

Each unit operates on its input in the usual manner so that

$$
\begin{aligned}
V_1 &= V_{\text{in}}\left(A_1\, e^{j\phi_1}\right)\\
V_2 &= V_1\left(A_2\, e^{j\phi_2}\right)\\
V_3 &= V_2\left(A_3\, e^{j\phi_3}\right)\\
&\text{etc.}
\end{aligned}
$$

so

$$\frac{V_{\text{out}}}{V_{\text{in}}} = (A_1 A_2 A_3 \ldots\ldots)\; e^{j(\phi_1+\phi_2+\phi_3+\ldots\ldots)}. \tag{8.16}$$

This expression shows that the final magnitude is determined by the product of the individual gains, while the net phase shift is the sum of the individual phase

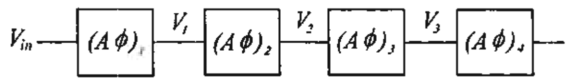

FIGURE 8.16. Cascaded modules, each with gain A and phase shift ϕ.

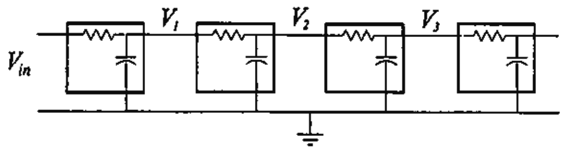

FIGURE 8.17. Cascaded first-order low-pass RC filters.

shifts. Noting that

$$20 \log (A_1 A_2 A_3 \ldots\ldots) = 20 \log A_1 + 20 \log A_2 + 20 \log A_3 + \ldots, \tag{8.17}$$

it is apparent that if the voltage ratio is measured in decibels, as defined by Eq. (5.34), then the effective gain for the chain is

$$G\,(\mathrm{dB}) = G_1 + G_2 + G_3 + \ldots\ldots . \tag{8.18}$$

Therefore, when measured in dB, the amplification (or attenuation) factors simply add.

Let us now apply these ideas using simple low-pass *RC* filter modules. To select a specific example, choose $R = 1\ \mathrm{k}\Omega$ and $C = 0.1\ \mu\mathrm{F}$ as in Fig. 8.2, and link the units together as in Fig. 8.17.

Actually, there is a slight problem here that must be addressed. As drawn in Fig. 8.17, any given segment will be loaded by the effect of the succeeding stages. In other words, the filters are not acting as a purely multiplicative chain in the spirit of Eq. (8.16) because each A is modified by the fact that additional circuitry is placed across its output. This can be corrected by inserting buffers between filter segments, as illustrated in Fig. 8.18.

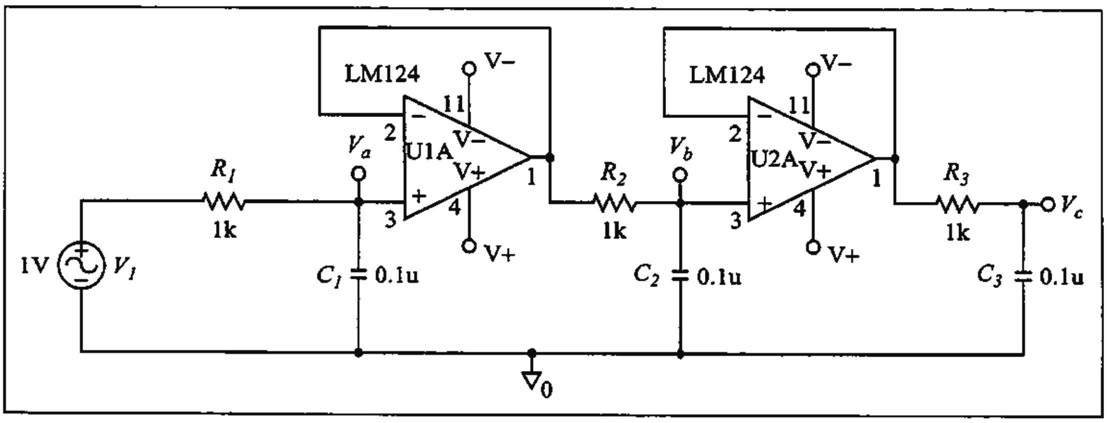

FIGURE 8.18. PSpice schematic of three cascaded first-order low-pass RC filters. The sections are separated by unity-gain buffers.

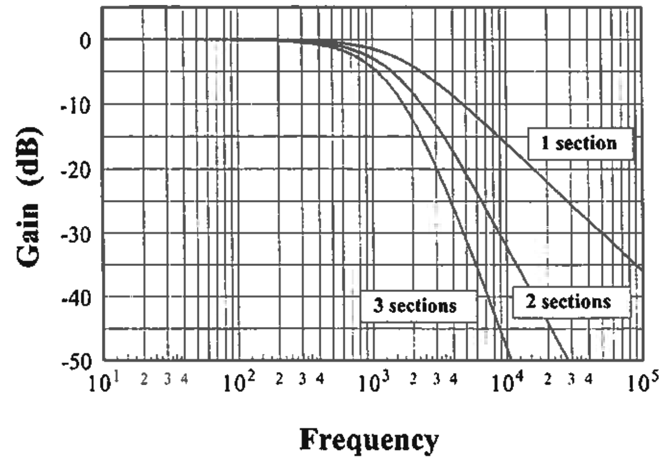

FIGURE 8.19. PSpice simulation results for the cascaded low-pass filters.

The PSpice outputs from each of the three stages V_a, V_b, and V_c are plotted in Fig. 8.19. The rolloffs are as anticipated, 20, 40, and 60 dB per decade (or 6, 12, and 18 dB per octave), indicating first-order, second-order, and third-order filter characteristics. Thus, the edges of the characteristic can be sharpened by adding filter stages.

Low-pass RLC filter

A second-order filter is created when two independent reactive components are present. In the last example, this was caused by the pair of capacitive blocks. A slightly different filter can be formed from series R and L, together with a shunting capacitance, as in Fig. 8.20. Then,

$$\frac{V_{\text{out}}}{V_{\text{in}}} = \frac{-\frac{j}{\omega C}}{R + j\omega L - \frac{j}{\omega C}} \tag{8.19}$$

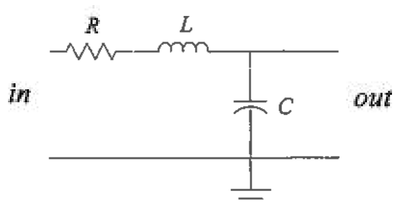

FIGURE 8.20. Second-order RLC filter.

or

$$\boxed{\frac{V_{\text{out}}}{V_{\text{in}}} = \frac{1}{(1-\omega^2 LC) + j(\omega RC)}}. \tag{8.20}$$

Suppose we define

$$\boxed{Q = \frac{1}{R}\sqrt{\frac{L}{C}}} \tag{8.21}$$

and

$$\boxed{\omega_0 = \frac{1}{\sqrt{LC}}}. \tag{8.22}$$

Then, Eq. (8.20) becomes

$$\frac{V_{\text{out}}}{V_{\text{in}}} = \frac{1}{\left(1-\left[\frac{\omega}{\omega_0}\right]^2\right) + j\left(\frac{\omega}{\omega_0}\frac{1}{Q}\right)}. \tag{8.23}$$

In this form, it is clear that although the circuit has three components, in fact there are only two independent variables: ω_0 and Q. The magnitude of the complex voltage ratio in Eq. (8.23) is

$$\left|\frac{V_{\text{out}}}{V_{\text{in}}}\right| = \frac{1}{\sqrt{\left(1-\left[\frac{\omega}{\omega_0}\right]^2\right)^2 + \left(\frac{\omega}{\omega_0}\frac{1}{Q}\right)^2}}. \tag{8.24}$$

The behavior of this function at high frequencies is dominated by the factor $[\frac{\omega}{\omega_0}]^4$, which occurs in the square root, and hence

$$\lim_{\omega\to\infty}\left|\frac{V_{\text{out}}}{V_{\text{in}}}\right| = \left(\frac{\omega_0}{\omega}\right)^2. \tag{8.25}$$

Noting then that $20\log|\frac{V_{\text{out}}}{V_{\text{in}}}|$ tends to $40\log(\frac{\omega_0}{\omega})$, the high-frequency rolloff is seen to be 40 dB per decade. Hence, this is a second-order low-pass filter.

For the components used in this example ($R = 1$ K, $L = 0.1$ H, $C = 0.1\ \mu$F), $Q = 1$ and $\omega_0 = 10^4$ ($f_0 = 1592$ Hz). The results from a PSpice simulation are shown in Fig. 8.21. Both decibel (left scale; solid curve) and linear (right scale;

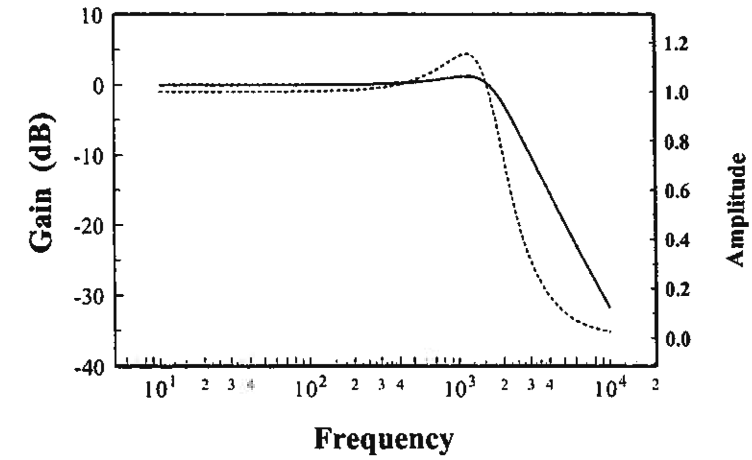

FIGURE 8.21. Frequency response of the RLC second-order low-pass filter showing the peak for $Q = 1$. The dashed curve is the same function but plotted with a linear scale (right) to bring out detail around the peak.

dashed curve) representations are given. The linear plot emphasizes the resonant peak in the filter function, whereas the logarithmic scaling reveals the expected rolloff at high frequencies.

8.2 ACTIVE FILTERS

Most of the passive filters just discussed were first-order—they utilized a single reactive element and possessed rolloffs of 20 dB per decade. More sharply defined pass- and stop-bands require higher-order circuits, which typically are of the active type. This is an extensive and complex topic, and we proceed by narrowing our focus to a single class of active filter named after R.P. Sallen and E.L. Key [1] but also commonly referred to as VCVS (voltage-controlled-voltage-source) circuits. First, the operating principles of a second-order active filter of this type will be developed, and then higher-order configurations will be presented.

Second-Order Filters

Low-pass

The basic arrangement of a second-order low-pass Sallen and Key active filter is shown in Fig. 8.22. From the schematic,

$$V_a - V_+ = I_a R_2, \tag{8.26}$$

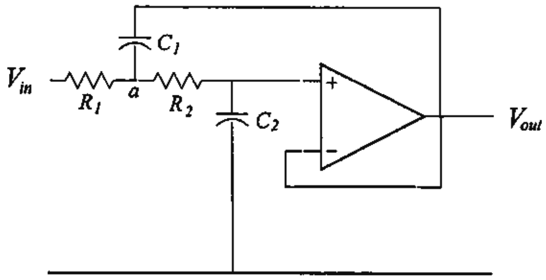

FIGURE 8.22. Second-order Sallen and Key low-pass active filter.

where I_a denotes the current flowing through resistor R_2 from node a towards the noninverting op-amp input. Because of the nearly infinite input impedance at this + node, I_a is constrained to flow through C_2, so $I_a = I_2$. Furthermore, the op-amp is wired as a unity-gain buffer, so $V_{\text{out}} = V_+$. Then, Eq. (8.26) becomes

$$V_a - V_{\text{out}} = I_2 R_2. \tag{8.27}$$

The current I_{in} in resistor R_1 satisfies

$$V_{\text{in}} - V_a = I_{\text{in}} R_1. \tag{8.28}$$

But also

$$I_2 = I_{\text{in}} + I_1. \tag{8.29}$$

Combining Eqs. (8.27)–(8.29),

$$V_{\text{in}} = V_{\text{out}} - I_1 R_1 + I_2 (R_1 + R_2). \tag{8.30}$$

To complete the derivation of the filter response, suitable expressions are needed for I_1 and I_2. These are easily obtained. The current in C_1 obeys

$$V_{\text{out}} - V_a = I_1 (-jX_1) \tag{8.31}$$

with $X_1 = \frac{1}{\omega C_1}$. Comparing Eq. (8.27) with Eq. (8.31),

$$I_1 = I_2 \left(-j \frac{R_2}{X_1}\right). \tag{8.32}$$

Likewise, the current in C_2 obeys

$$V_{\text{out}} = V_+ = I_2(-jX_2), \tag{8.33}$$

so

$$I_2 = j\frac{V_{\text{out}}}{X_2}, \tag{8.34}$$

where $X_2 = \frac{1}{\omega C_2}$ is the capacitive reactance.

Finally, substituting Eqs. (8.32) and (8.34) into Eq. (8.30),

$$V_{\text{out}} = V_{\text{in}}\left[\left(1 - \frac{R_1R_2}{X_1X_2}\right) + j\left(\frac{R_1+R_2}{X_2}\right)\right]^{-1}. \tag{8.35}$$

Thus,

$$\boxed{\frac{V_{\text{out}}}{V_{\text{in}}} = \frac{1}{[1-\omega^2R_1R_2C_1C_2] + j[\omega C_2(R_1+R_2)]}}. \tag{8.36}$$

Notice the exact correspondence in form between this equation and Eq. (8.20), which was developed from a second-order passive *RLC* filter. In other words, this active low-pass filter, which contains only resistors and capacitors, effectively simulates an equivalent inductance. Generally speaking, capacitors are preferred over inductors as circuit components because of their wide availability, low cost, and small size.

Equations (8.20) and (8.36) point to the correspondences

$$LC \Leftrightarrow R_1R_2C_1C_2$$

$$RC \Leftrightarrow C_2(R_1+R_2)$$

from which, and employing Eqs. (8.21) and (8.22),

$$\boxed{Q = \frac{\sqrt{R_1R_2C_1}}{\sqrt{C_2}\,(R_1+R_2)}}, \tag{8.37}$$

$$\boxed{\omega_0 = \frac{1}{\sqrt{R_1R_2C_1C_2}}}. \tag{8.38}$$

The circuit of Fig. 8.22 is commonly generalized by the addition of gain-setting resistors R_3 and R_4, as shown in Fig. 8.23. Now, the op-amp is wired as

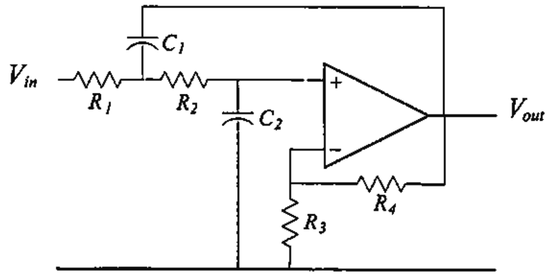

FIGURE 8.23. Second-order active low-pass filter with gain-setting resistors added.

a noninverting amplifier with closed-loop gain $G = 1 + \frac{R_4}{R_3}$. This changes the result of Eq. (8.36) to [2]

$$\frac{V_{\text{out}}}{V_{\text{in}}} = \frac{G}{\left[1 - \omega^2 R_1 R_2 C_1 C_2\right] + j\left[\omega R_1 C_1 (1 - G) + \omega C_2 (R_1 + R_2)\right]}, \tag{8.39}$$

which of course returns to the earlier result when $G = 1$. The filter ω_0 is still given by Eq. (8.38), but the Q changes somewhat to

$$Q = \frac{\sqrt{R_1 R_2 C_1 C_2}}{R_1 C_1 (1 - G) + C_2 (R_1 + R_2)}. \tag{8.40}$$

In a practical sense, there are too many adjustable parameters in these equations. That is, there are seemingly infinitely many ways of achieving any given filter response. A usable design process must narrow the options in some reasonable fashion.

Normalized filters

The following is one of several standardized schemes for defining a canonical Sallen and Key low-pass filter [3]. Let $R_1 = R_2 = 1\ \Omega$. Specify the corner frequency of the normalized filter as $\omega_c = 1$ radian/sec (ω_c will equal ω_0 in some cases, but not generally). Let $R_3 = \infty$ and $R_4 = 0$, so that $G = 1$. Even with all these restrictions, there remain infinitely many acceptable pairs C_1, C_2, but certain precise combinations lead to especially desirable filter characteristics. The significance of some choices is illustrated in Fig. 8.24. The curve that results from $C_1 = 1.414$ F and $C_2 = 0.707$ F rolls off smoothly, dropping to $\frac{1}{\sqrt{2}}$ (i.e., -3 dB) at the corner frequency $f_c = 1/2\pi = 0.159$ Hz. In fact, these particular component values happen to satisfy the criterion of maximal flatness within the passband; this is known as a *Butterworth filter*. The detailed procedures for deducing capacitance and/or resistance values from conditions on

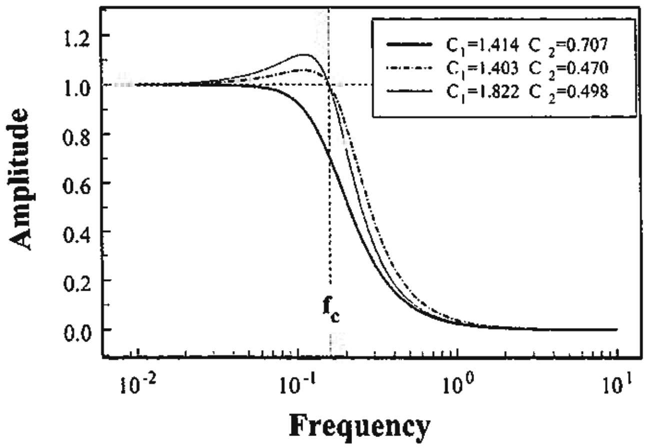

FIGURE 8.24. Frequency response of second-order active low-pass filter illustrating Butterworth (smooth lower curve) and Chebyshev (peaked) characteristics.

flatness, or from polynomial properties (next paragraph), constitute a lengthy and specialized topic for which the reader is directed to other sources [3, 4, 5].

The two other curves in the figure exhibit a peaked response. For the capacitance values selected, these are second-order *Chebyshev filter* characteristics (also known as equal ripple), and they achieve an increased abruptness in falloff by paying the price of ripple in the passband. By permitting larger ripple, the transition region can be narrowed, as the figure illustrates.

For these two cases, as shown in the logarithmically scaled plot of Fig. 8.25, the peak amplitude is 0.5 dB when $C_1 = 1.403$ F and $C_2 = 0.470$ F, and is 1.0 dB when $C_1 = 1.822$ F and $C_2 = 0.498$ F. As expected for second-order filters, the

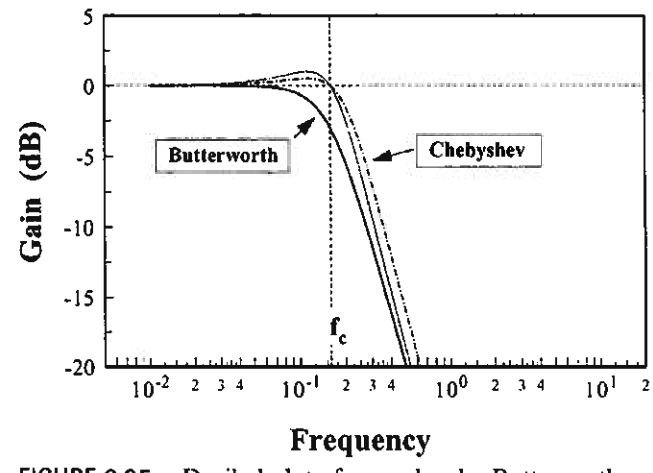

FIGURE 8.25. Decibel plot of second-order Butterworth and Chebyshev filter characteristics. Well beyond the corner frequency, the rolloff is 40 dB per decade.

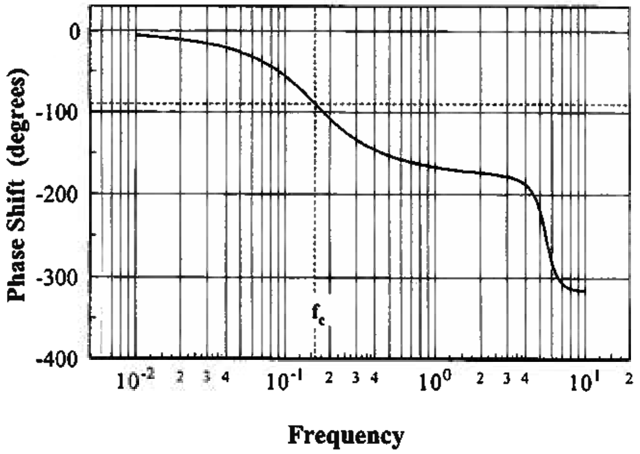

FIGURE 8.26. Phase shift in a second-order Butterworth low-pass filter.

high-frequency rolloff is 40 dB per decade. Note that for the Chebyshev filter, the frequency f_c is not the place at which the rolloff has dropped the amplitude by 3 dB, as is the case for second-order Butterworth and first-order passive filters, but rather it marks the end of the ripple zone.

To be more precise, f_c is defined for the Chebyshev characteristic as the frequency at which the response drops below the ripple band. For even-order filters (2nd order, 4th order, etc.), the ripple consists of one or more peaks which lie entirely above the 0 dB level. In odd-order Chebyshev filters (3rd order, 5th order, etc.), the ripple lies entirely below the 0 dB level. An example illustrating this property is given in the section on third-order filters.

The phase response of a second-order Butterworth filter is shown in Fig. 8.26.

The following table summarizes results from this section (remember that $R_1 = R_2 = 1.0\ \Omega$).

	C_1(F)	C_2(F)	ω_0(sec^{-1})	Q
Butterworth	1.41421	0.70711	1.0	0.7071
Chebyshev 0.5 dB	1.40259	0.47013	1.2315	0.8636
Chebyshev 1.0 dB	1.82192	0.49783	1.0500	0.9565

Design example

All of the preceding capacitor combinations C_1, C_2 in Farads are for normalized filters with a corner frequency of 1 radian/sec and $R_1 = R_2 = 1\ \Omega$. Suppose a second-order low-pass Butterworth filter is desired, which has a corner frequency of 1500 Hz. The filter characteristic can be scaled appropriately upward in frequency if the normalized Butterworth capacitors $C_1 = 1.41421$ F and

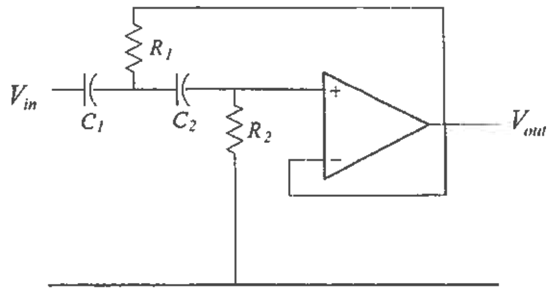

FIGURE 8.27. Second-order high-pass active filter.

$C_2 = 0.70711$ F are each made smaller by the desired factor of 2π (1500). This gives new values $C_1 = 1.501 \times 10^{-4}$ F and $C_2 = 7.503 \times 10^{-5}$ F. At this point, it is possible to rescale the two resistors from their original 1 Ω values to something more reasonable, such as perhaps 10 kΩ. The new corner frequency can be left unaffected after magnifying the resistors if the capacitors are divided by the same numerical factor (in this case 10^4). Hence, we arrive at the final filter values: $R_1 = 10$ K, $R_2 = 10$ K, $C_1 = 15.01$ nF, $C_2 = 7.503$ nF.

High-pass

High-pass active filters can be created simply by interchanging the roles of resistors and capacitors in a manner reminiscent of the passive *RC* circuit. Thus, Fig. 8.27 represents a second-order, high-pass Sallen and Key design. The following table gives the component values for several filter types. In these cases, $C_1 = C_2 = 1.0$ F and the corner frequency is again normalized to $\omega_c = 1.0$ radian/sec.

	$R_1(\Omega)$	$R_2(\Omega)$	$\omega_0(\sec^{-1})$	Q
Butterworth	0.70711	1.41421	1.0	0.4714
Chebyshev 0.5 dB	0.71281	2.12707	0.8121	0.4336
Chebyshev 1.0 dB	0.54586	2.00872	0.9550	0.4099

As an example of an active high-pass circuit, Fig. 8.28 shows the frequency response of the normalized 1.0 dB Chebyshev filter as specified by the resistor values in the third line of the table.

Band-pass

The general layout for a second-order Sallen and Key band-pass filter is shown in Fig. 8.29. One normalizing scheme [3] that is suitable is to set $C_1 = C_2 = 1.0$ F. Further, set $R_1 = 1.0\ \Omega$. The gain of the amplifier is of course $G = 1 + \frac{R_4}{R_5}$, so only the ratio $\frac{R_4}{R_5}$ together with R_2 and R_3 remain as undetermined quantities.

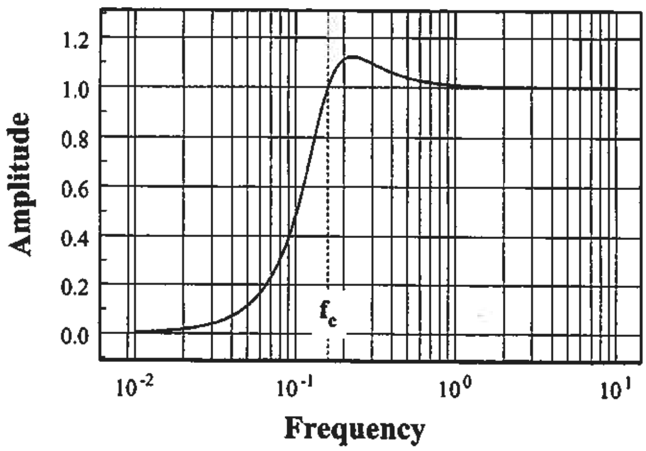

FIGURE 8.28. Second-order 1.0 dB Chebyshev high-pass filter frequency response.

Choose $R_4 = R_5$. It is desired to have the center frequency of the passband equal to unity: $\omega_c = 1.0$ radian/sec. The following table shows some possible choices for the remaining resistors and the resulting values of Q.

$R_2(\Omega)$	$R_3(\Omega)$	Q
0.74031	2.35078	2
0.63439	2.57630	5
0.60471	2.63567	10

The parameter Q measures the sharpness of the peak and is defined as the ratio $\frac{\omega_c}{\Delta\omega}$, where ω_c, as above, is the center frequency and $\Delta\omega$ is the peak width.

Design example

Using the first line in the table, we can design a filter with a center frequency of, say, 500 Hz and a Q of 2 as follows. The normalized filter has a center

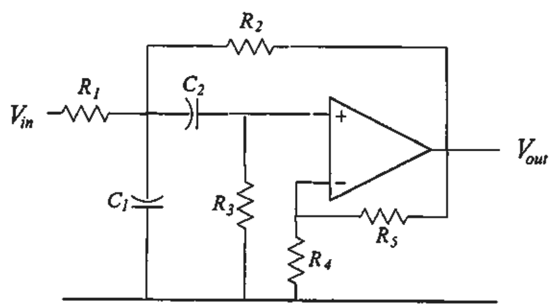

FIGURE 8.29. Second-order Sallen and Key band-pass filter.

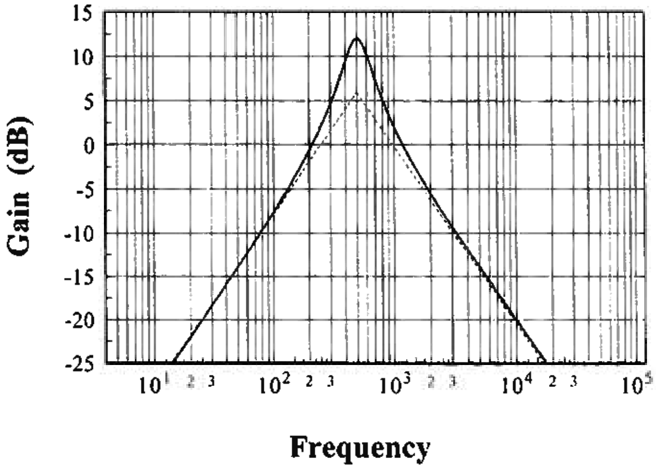

FIGURE 8.30. Second-order active band-pass characteristic with center frequency at $f_c = 500$ Hz.

frequency of $f_c = \frac{\omega_c}{2\pi}$ with $\omega_c = 1$. Thus, to raise the center frequency to 500, the capacitors should be scaled by $\frac{1}{2\pi \times 500}$ so $C_1 = C_2 = 318.31\ \mu$F. To maintain the new center frequency but adjust the capacitors to somewhat more realistic values, let us divide the C's by 1000 and at the same time multiply the resistors by 1000. The filter now is specified by $C_1 = C_2 = 0.31831\ \mu$F, $R_1 = 1$ kΩ, $R_2 = 740\ \Omega$, $R_3 = 2.351$ kΩ. Only the ratio of the gain-setting resistors matters, so choose $R_4 = R_5 = 1$ kΩ. The resulting filter characteristics are plotted in Fig. 8.30.

The dashed lines indicate the linear 20 dB per decade rolloff of the filter at low and high frequencies. For this design, $G = 2$, which is 6.02 dB. Note that the two linear extrapolations intersect at the point (500 Hz, 6.02 dB). The actual filter characteristic rises above this in a $Q = 2$ peak.

The effect of higher Q filters is illustrated in Fig. 8.31, where progressively narrower pass-bands appear. A linear vertical scale has been chosen here so that the peak effect is clearly revealed. These frequency response characteristics could appropriately be considered as defining "slot" filters (the inverse of notch filters), which are transparent to only a very restricted range of frequencies. Such a property can in fact be useful in particular applications where a nearly monochromatic "signal" is surrounded by extraneous noise.

Third-Order Filters

A third-order Sallen and Key low-pass filter is illustrated in Fig. 8.32. Adopting, as before, a normalized filter (corner frequency $\omega_c = 1.0$) with $R_1 = R_2 = R_3 = 1.0\ \Omega$, the required capacitor values are given in the following table.

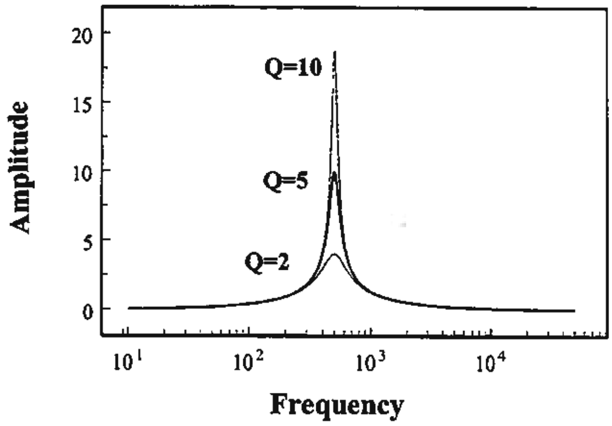

FIGURE 8.31. Second-order active band-pass filters with center frequency of 500 Hz and Q values of 2, 5, and 10.

	C_1(F)	C_2(F)	C_3(F)
Butterworth	0.20245	3.5465	1.3926
Chebyshev 1 dB	0.05872	14.784	2.3444

PSpice simulations for both Butterworth and 1.0 dB Chebyshev filters using component values as specified in the table produce the results plotted in Fig. 8.33. As expected for a third-order low-pass filter, the high-frequency rolloff is quite steep at 60 dB per decade (18 dB per octave).

As might be anticipated, a third-order high-pass filter can be derived from the low-pass circuit (Fig. 8.32) by interchanging the roles of resistor and capacitor. Hence, with $C_1 = C_2 = C_3 = 1.0$ F, the design table for normalized characteristics is

	$R_1(\Omega)$	$R_2(\Omega)$	$R_3(\Omega)$
Butterworth	4.93949	0.28194	0.71808
Chebyshev 1 dB	17.0299	0.06764	0.42655

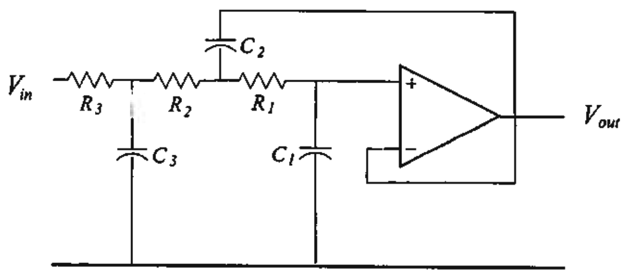

FIGURE 8.32. Third-order active Sallen and Key low-pass filter.

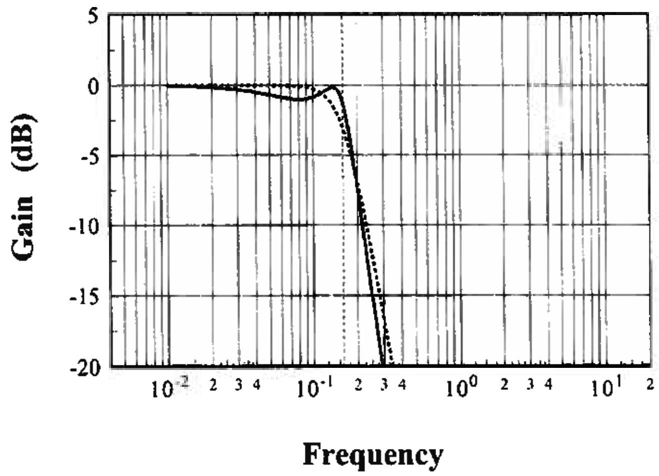

FIGURE 8.33. Frequency response of third-order active low-pass filter. Both Butterworth (dashed) and 1 dB Chebyshev (solid) characteristics are shown.

8.3 REMARKS

This chapter has provided an introduction to the basic concepts of analog filters. For all but the simplest applications, active filters are probably the best choice. Second- or third-order designs are generally sufficient.

The decision regarding tradeoffs is not always cut-and-dried, although in many instances the instrumentation application itself will dictate some choices—low ripple versus narrow transition region, low-order filter design versus sharply defined bands.

Active filter circuits are typically overdetermined in the sense that there are more variables (component values) than constraints. This allows some components to be preset to convenient values while the remaining ones are determined so that the real filter behaves as much as possible like the ideal target. The component values presented in the previous tables were specific to a particular normalizing scheme. The appropriate values were simply quoted (see [3]) without proof.

The actual method of determining correct component values is a complicated business, and the reader is referred to specialized texts for details. However, a simple example will at least illustrate the process.

Consider the general second-order active low-pass filter, as illustrated in Fig. 8.23. From Eq. (8.39) the circuit response can be written in the form

$$\frac{V_{\text{out}}}{V_{\text{in}}} = \frac{G}{[R_1 R_2 C_1 C_2]\ s^2 + [R_1 C_1 (1 - G) + (R_1 + R_2) C_2]\ s + 1} \qquad (8.41)$$

with $s \equiv j\omega$. In more compact form,

$$\frac{V_{\text{out}}}{V_{\text{in}}} = \frac{Gb_0}{s^2 + b_1 s + b_0}, \tag{8.42}$$

where

$$b_0 = \frac{1}{R_1 R_2 C_1 C_2} \tag{8.43}$$

and

$$b_1 = \frac{R_1 C_1 (1 - G) + (R_1 + R_2) C_2}{R_1 R_2 C_1 C_2}. \tag{8.44}$$

A Butterworth polynomial of nth order can be expressed

$$T(s) = \frac{1}{a_n s^n + a_{n-1} s^{n-1} + \cdots + a_2 s^2 + a_1 s^1 + 1}. \tag{8.45}$$

The coefficients of these polynomials have been tabulated (see [5], p. 69) and are, for the case $n = 2$, $a_1 = \sqrt{2}$ and $a_2 = 1$. To produce a Butterworth filter, the circuit response function [Eq. (8.41) or Eq. (8.42)] must be made to match the polynomial, term by term.

For a normalized filter with $G = 1$, we wish to have $\omega_0 = 1$, and this just requires $b_0 = 1$ or

$$R_1 R_2 C_1 C_2 = 1. \tag{8.46}$$

The remaining condition needed to guarantee a match with the Butterworth polynomial is $a_1 = b_1 = \sqrt{2}$, which forces

$$(R_1 + R_2) C_2 = \sqrt{2}. \tag{8.47}$$

Notice that there are only two constraints—Eqs. (8.46) and (8.47)—but four components to be determined. In the earlier discussion of this second-order low-pass filter, an additional arbitrary but convenient choice was made: $R_1 = R_2 = 1.0\ \Omega$. With the resistors fixed, the capacitors must then be $C_2 = \frac{\sqrt{2}}{2} = 0.70711$ and $C_1 = \frac{1}{C_2} = 1.41421$. These are precisely the component values listed in the table accompanying the earlier discussion of the low-pass Butterworth filter.

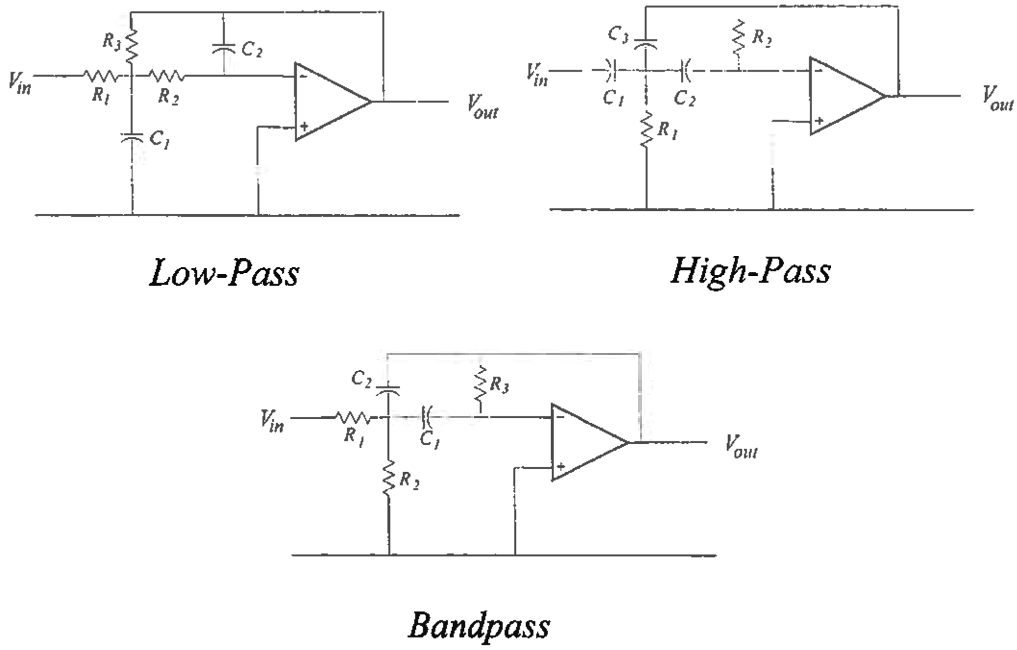

FIGURE 8.34. Configurations for second-order multiple feedback (MFB) active filters.

A third-order filter can be analyzed in a similar fashion knowing that the Butterworth coefficients are $a_1 = 2$, $a_2 = 2$, and $a_3 = 1$ (see [5], Table 8-3, p. 69).

Higher-order filters, as well as other types (Chebyshev, Elliptic, Bessel, etc.) based on different polynomials, require much more algebraic effort. These tasks are normally carried out on computers, and specialized software is now available to facilitate interactive filter design. Although such methods may be necessary for demanding applications, standard reference texts which are available in most engineering libraries provide concise summaries of design data that are usually adequate for most situations.

Although the discussion has been restricted to Sallen and Key (VCVS) circuits, it should be noted that other active filter designs are possible. The most common alternative to VCVS is the so-called Multiple Feedback (MFB) arrangement shown in Fig. 8.34. These filters are discussed in [3, 4, 5, 2, 7].

PROBLEMS

Problem 8.1. The discussion of passive first-order filters included low-pass RC, low-pass RL, and high-pass RC. A fourth possibility would be a high-pass RL filter. Design such a filter with the following characteristics: $f_c = 2$ kHz and

$R = 1\ \mathrm{k}\Omega$. If possible, verify the final design with PSpice or a similar simulation package.

Problem 8.2. Design an active second-order, low-pass 1.0 dB Chebyshev filter using 5 kΩ resistors such that the corner frequency is 2 kHz. If possible, verify the final design with PSpice or a similar simulation package.

BIBLIOGRAPHY

[1] R.P. Sallen and E.L. Key, "A practical method of designing RC active filters," IRE Trans. Circuit Theory 2, 74–85, March (1955).

[2] Martin Hartley Jones, *A Practical Introduction to Electronic Circuits* (Cambridge University Press, Cambridge, U.K., 1977), pp. 162–170.

[3] Z.H. Meiksin, *Complete Guide to Active Filter Design, Op Amps, and Passive Components* (Prentice-Hall, Englewood Cliffs, NJ 1990); see in particular Table 3-1.

[4] David E. Johnson and John L. Hilburn, *Rapid Practical Designs of Active Filters* (John Wiley & Sons, New York 1975); see in particular Tables 2-2 through 2-7.

[5] Carson Chen, *Active Filter Design* (Hayden Book Company, 1982).

[6] William D. Stanley, *Operational Amplifiers with Linear Integrated Circuits*, third edition (Merrill/Macmillan College Publishing Company, New York 1994), Chapter 8.

[7] Thomas L. Floyd, *Fundamentals of Linear Circuits* (Merrill/Macmillan College Publishing Company, New York 1992), p. 388.

[8] J.D. Turner, *Instrumentation for Engineers* (Macmillan Education Ltd., New York 1988), Chapter 4.

[9] Stephen E. Derenzo, *Interfacing: A Laboratory Approach Using the Microcomputer for Instrumentation, Data Analysis, and Control* (Prentice-Hall, Englewood Cliffs, NJ 1990), pp. 62–71.